JCTC Journal of Chemical Theory and Computation

Article

pubs.acs.org/JCTC

Origin of the Red Shift for the Lowest Singlet $\pi \rightarrow \pi^*$ Charge-Transfer Absorption of *p*-Nitroaniline in Supercritical CO_2

Marcelo Hidalgo,[†] Roberto Rivelino,*[,†,‡] and Sylvio Canuto*[,†]

[†]Instituto de Física, Universidade de São Paulo, CP 66318, 05314-970 São Paulo, SP Brazil

[‡]Instituto de Física, Universidade Federal da Bahia, 40210-340 Salvador, Bahia Brazil

ABSTRACT: The origin of the unusual solvatochromic shift of *p*-nitroaniline (PNA) in supercritical carbon dioxide ($SCCO_2$) is theoretically investigated on the basis of experimental data. Ab initio quantum chemistry calculations have been employed to unveil the interaction of CO_2 with this archetypical molecule. It is demonstrated that the nitro group of PNA works as an electron-donating site binding to the electron-deficient carbon atom of CO_2, most probably via a Lewis acid−base interaction. Moreover, a cooperative C−H···O hydrogen bond seems to act as an additional stabilizing source during the solvation process of PNA in $SCCO_2$. To support the influence of solute−solvent specific interactions on the lowest singlet $\pi \rightarrow \pi^*$ charge-transfer excitation, we perform a sequential Monte Carlo time-dependent density functional theory simulation to evaluate the excited states of PNA in $SCCO_2$ (T = 315 K, ρ = 0.81 g/cm^3). A critical assessment of this simulation, compared to calculations carried out within the polarized continuum model, gives strong evidence that our proposed complexes are important in describing the solvatochromic shift of PNA in $SCCO_2$. The calculated red shift from the gas phase accounts for 66% to 80% (depending on the degree of complexation) of the experimental data. Finally, these results also alleviate possible failures commonly attributed to long-range corrected functionals in reproducing the solvatochromism of PNA.

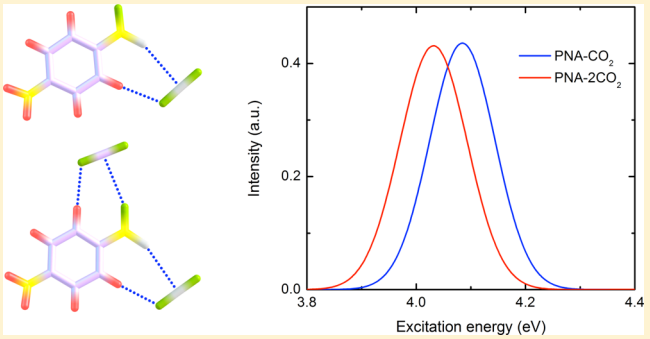

1. INTRODUCTION

Supercritical fluids are ideal substitutes of common organic solvents in several processes on industrial and laboratory scales, due to their unique thermophysical properties.[1] Considering the inertness, low polarity, and suitable critical constants, supercritical carbon dioxide ($SCCO_2$) has successfully been employed in fields ranging from green extraction techniques[2,3] to dye processes.[4] Moreover, solubility of molecules in $SCCO_2$ is an issue of great interest for understanding the supercritical fluid process[5] as well as the role of specific solute−solvent interactions.[6,7] In this sense, recent studies[5] on the high-pressure solvation equilibrium processes of *p*-nitroaniline (PNA) in $SCCO_2$ have demonstrated that its solubility increases by increasing the pressure at constant temperature. Additionally, this equilibrium solubility is slightly enhanced when a nonpolar cosolvent is employed in the solvation process.[5] These findings indicate that although PNA is a high polarity molecule, which is a prototypical azoic dye, it is unusually soluble in $SCCO_2$. Therefore, specific solute−solvent interactions should play an important role in enhancing the solubility of PNA in $SCCO_2$.

Specific intermolecular interactions of CO_2 with materials containing electron-donating functional groups has long been recognized as a Lewis acid−base (LA−LB) type complexation.[8,9] This is usually characterized by the interaction between the electron deficient carbon of CO_2 and, e.g., the electron lone pairs of a carbonyl oxygen atom of the interacting system.[7,10] In some CO_2-philic compounds, a LA−LB interaction may be accompanied by a weaker, although cooperative, C−H···O hydrogen bond, acting as an additional stabilizing source during the solvation process of CO_2-philes with hydrogen atoms attached to an α-carbon.[11] Furthermore, these kinds of interactions have been proposed and theoretically characterized in formaldehyde complexes with HCN and FCN, which are similar to the corresponding CO_2 complex.[12] Recently, LA−LB interactions have also been investigated for a variety of organic molecules, including distinct functional groups,[13,14] from ab initio calculations. Because of the chemical and engineering implications of this specific interaction involving a nonpolar solvent such CO_2, it is timely to understand the basic principles for designing other CO_2-philic compounds under supercritical conditions.[15]

An interesting family of molecules exhibiting a rather electron-rich group, but that appears not to be exploited as CO_2-philic species, is the chemical group of aromatic nitrocompounds. Among this group, nitroanilines—π-conjugated donor−acceptor or "push−pull" molecules—have great interest because of their large nonlinear optical responses[16] and intramolecular charge-transfer (CT) electronic excitations,

Received: December 13, 2013
Published: March 6, 2014

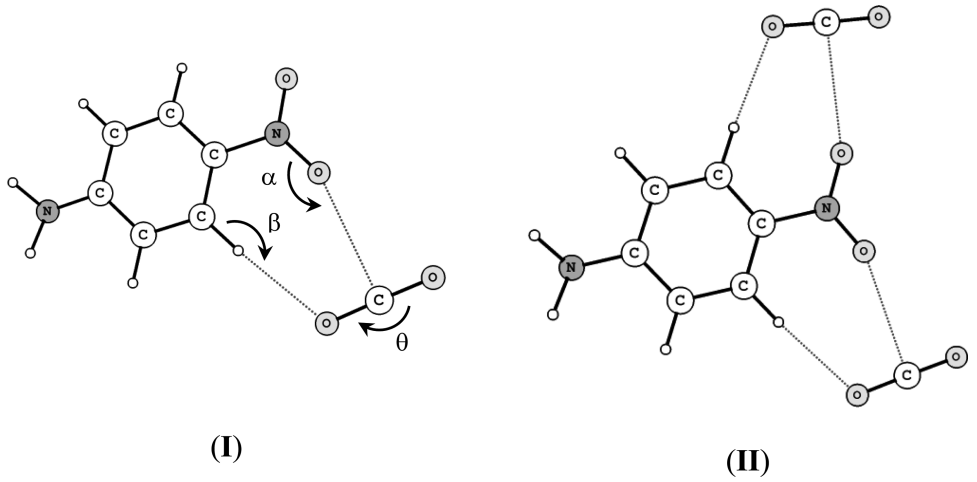

Figure 1. Illustration of the optimized structures of the LA−LB complexes as obtained from MP2/aug-cc-pVDZ: (**I**) PNA-CO_2 and (**II**) PNA-$2CO_2$.

which are strongly dependent on the local solvent environment.[17−20] For example, there is currently considerable interest in the solvent-induced changes on the spectral properties of PNA, for which the vibronic coupling of the symmetric ⟩C−NO_2 stretching contribution exerts an important influence on the electronic absorption spectrum.[17,21,22] Dreyer and coworkers[23] have found a good correlation between the vibrational frequency shifts and the lowest singlet $\pi \rightarrow \pi^*$ CT electronic absorption of PNA in solvents with different polarities. Many other recent studies[24−26] have investigated the solvent-induced shift of this absorption band of PNA in water, although none of them seems to have heeded the role of specific solute−solvent interactions under supercritical conditions. Only, Frutos-Puerto et al.[27] have attributed the nonlinear solvatochromic shift of PNA in cyclohexane−triethylamine mixtures, under usual thermodynamic conditions, to the possible hydrogen bond formation with the amino group.

In the present paper, motivated by the high-pressure equilibrium solubility study[5] of PNA in $SCCO_2$, as well as the relatively high solvatochromic shift of the CT electronic transition observed for PNA under supercritical conditions,[28,29] we employ different levels of theory to understand the fundamental principles behind the interaction of CO_2 and PNA. First, we investigate the possibility of this highly polarizable molecule to form LA−LB complexes, in the same sense in which carbonyl systems can form them, by employing ab initio quantum chemistry methods. Second, we simulate the supercritical conditions of CO_2 to obtain the structural feature of the first solvation shells around PNA via classical Monte Carlo method. Third, we utilize statistically uncorrelated structures of PNA in $SCCO_2$ for sequential QM/MM calculations[30−35] to assess the lowest singlet electronic absorption spectrum. Our results give evidence that formation of LA−LB interactions, along with cooperative C−H···O bonds, may explain the good solubility and unusual red shift observed for PNA in $SCCO_2$ from its gas phase.

2. METHODS AND COMPUTATIONAL PROCEDURES

The calculations to investigate the proposed LA−LB CO_2 complexes of PNA (see Figure 1) in this work have been carried out using the Møller−Plesset partitioning method[36] truncated at the second order (MP2), as implemented in the Gaussian 09 program.[37] The augmented correlation-consistent basis set with polarized valence of double-ζ quality (aug-cc-pVDZ)[38] was employed as a compromise between accuracy and computational feasibility.[27] Stationary points were found by performing complete geometry optimizations at the MP2/aug-cc-pVDZ level within the supermolecular approach, starting with initial planar geometrical arrangements in C_s symmetry. Interaction energies were calculated taking into account corrections for basis set superposition error (BSSE)[39] through the counterpoise (CP) technique.[40] Population analysis and electrostatic potentials were properly obtained through the MP2 electron densities, with maps generated over a grid of 77 × 77 × 77 points for further visualization.

Frequency calculations within the harmonic approximation were also performed to obtain the vibrational spectra (infrared and Raman intensities) and zero-point vibrational energies (ZPVE) of the complexes at the MP2/aug-cc-pVDZ level of theory. Raman light-scattering properties were also calculated within this level for the most prominent Raman bands. The differential cross sections of depolarized Raman scattering observed at right angles to the incident beam are determined by the activities,[41] whereas the depolarization ratios for both natural and plane-polarized light are, respectively, given by

$$\rho_n = \frac{6(\Delta\alpha')^2}{45(\bar{\alpha}')^2 + 7(\Delta\alpha')^2} \quad (1)$$

$$\rho_p = \frac{3(\Delta\alpha')^2}{45(\bar{\alpha}')^2 + 4(\Delta\alpha')^2} \quad (2)$$

where $\bar{\alpha}'$ and $\Delta\alpha'$ are the derivatives of the average and anisotropic dipole polarizabilities.[41] The largest values of the depolarization ratios arise for the most depolarized band, varying in the $0 < \rho_n < (6/7)$ and $0 < \rho_p < (3/4)$ ranges. These are useful properties to identify possible changes in the vibrational modes due to complexation. All of these calculations were also performed within density functional theory using the hybrid functional B3LYP.[42]

The lowest singlet $\pi \rightarrow \pi^*$ electronic excited state of PNA and its LA−LB complexes was calculated within schemes of time-dependent density functional theory (TD-DFT).[43,44] To describe the electronic absorption of PNA in the gas phase, we started from its MP2-optimized geometry and considered the long-range corrected functional CAM-B3LYP functional (LC-DFT),[45] combined with the aug-cc-pVDZ basis set. We have chosen this density functional because it has better reproduced

dx.doi.org/10.1021/ct401081e | J. Chem. Theory Comput. 2014, 10, 1554−1562

the electronic transitions of PNA than regular hybrid B3LYP, as compared to its gas phase spectrum. Furthermore, as recently reported in ref 15, LC-DFT functionals are strongly recommended for describing the nonlinear optical properties of this prototypical chromophore. Although we are aware of the possible limitations of these functionals in describing the solvatochromic shift of the lowest intramolecular CT excitation of PNA in water,[24,26] we cannot proceed without TD-DFT for a large number of explicit solvent molecules included in the excited state calculations. As a first approximation to evaluate the effect of $SCCO_2$ on the absorption spectrum of PNA, we have combined TD-CAM-B3LYP with the polarizable continuum model (PCM)[46] using dielectric constant[47] $\varepsilon = 1.5$, which was determined for the supercritical conditions of CO_2. To describe the charge redistribution of PNA in the solvent medium, we also considered the MP2 reoptimized geometries within PCM.[46] Furthermore, we calculated the spectra of the CO_2 complexes of PNA in PCM ($\varepsilon = 1.5$) following the same prescription used for a single molecule, i.e., MP2(PCM)//CAM-B3LYP/aug-cc-pVDZ.

The effect of explicit CO_2 molecules under supercritical conditions was also taken into account to investigate the lowest singlet excitation of PNA, by employing the sequential QM/MM method (S-QM/MM).[30−35] Hence, performing a classical Monte Carlo simulation with Lennard-Jones, Coulomb, and geometric parameters proposed in ref 48, which reproduce the critical point of CO_2, we obtained statistically uncorrelated configurations[31,34] of one PNA molecule in 500 CO_2 molecules, at a temperature of 315 K and density of 0.81 g/cm^3. The absorption spectrum experimentally measured for PNA in $SCCO_2$ is known from these conditions in the literature.[28] To carry out the S-QM/MM scheme, we have considered two ways: (i) one PNA within an embedding of 350 point charges representing the CO_2 solvent molecules and (ii) one PNA plus 12 explicit CO_2 molecules within an embedding of 350 point charges. Finally, the excitation energy in QM partitioning was calculated within TD-CAM-B3LYP/aug-cc-pVDZ.

3. RESULTS AND DISCUSSION

3.1. Structure, Energetics, and Vibration Analysis of the PNA-CO_2 Complexes. The two optimized structures of the CO_2 complexes formed with PNA are displayed in Figure 1, as proposed in this work. These complexes are supposed to be mostly stabilized by Lewis acid−base interactions (LA−LB), involving the nitro group oxygen atom and the electron-deficient carbon atom in CO_2. This assumption is noticed by the presence of the N−O···C bond formed in complexes **I** and **II**, which exhibit a characteristic geometry of LA−LB complexation, similar to some extent to that occurring in carbonyl compounds with CO_2.[6,7,12]

It is also possible to identify a nonconventional H-bond interaction of the C−H···O type, shared with a first neighbor hydrogen to the nitro group in the aromatic ring of PNA and one of the oxygen atoms of CO_2. However, a description based purely on geometric features is rather approximated to support these intermolecular interactions. As we will discuss later, based on the energetics and vibrational spectra, this H-bond acts cooperatively[39] along with the LA−LB interaction, increasing the stability of the resultant complexes, since formation of the N−O···C bond removes electron density from the PNA subunit, making it a more powerful proton donor near the nitro group.

All necessary geometric parameters to characterize these intermolecular bonds are displayed in Figure 1, and the optimized parameters for both complexes are given in Table 1.

Table 1. Geometric Parameters[a] Optimized at the MP2/aug-cc-pVDZ Level for the PNA-CO_2 Complexes (Angles in Degrees and Distances in Å)

angles	complex **I**	complex **II**
θ	178.91	178.93
$\Delta\theta$	1.09	1.07
α (N−O···C)	158.37	158.30
β (C−H···O)	176.46	176.55
distances	complex **I**	complex **II**
C−H (H-bonded)	1.091	1.091
Δ(C−H)	0.000	0.000
N−O (LA−LB)	1.241	1.241
Δ(N−O)	0.001	0.001
N═O	1.240	
C═O (H-bonded)	1.182	1.182
C═O	1.178	1.178
NO···C	2.890	2.894
CH···O	2.366	2.358

[a]See Figure 1 for identifying labels.

The more emblematic parameters are the intermolecular bond angles (α and β), the covalent bond angle (θ) of CO_2, the intermolecular distance (C···O), and the H-bond distance (H···O), which are used to assess the nature of the interactions. As in the case of other LA−LB complexes, the calculated values indicate the presence of weak C−H···O interactions, with a H···O distance of around 2.36 Å and $\beta \cong 176°$, acting cooperatively to stabilize both PNA-CO_2 complexes. In turn, the calculated O···C distance is around of 2.89 Å in complex **I**, with a slight increase of 4 mÅ in complex **II**, and the characteristic angle (α) of the LA−LB interaction is around 158°. These values are also in agreement with typical LA−LB complexes.[6,7,10] Furthermore, small changes in the covalent parameters occur upon the complex formation.

A typical aspect in this interaction is that the CO_2 molecule becomes slightly bent after being bound, exhibiting a deformation of ca. 1.1° from its linear shape in both complexes. As we will discuss in the following, this structural deformation results in the splitting of the doubly degenerate vibrational bending mode, ν_2, upon its complexation with PNA. As first noticed for LA−LB complexes with CO_2,[9] the splitting of the ν_2 mode has been used as a signature for characterizing these types of complexes. As demonstrated in ref 12, the splitting in degenerate vibrational modes of small linear molecules involved in LA−LB complexation is related to the strength of the interaction. Accordingly, for complexes **I** and **II** studied here, this frequency splitting in CO_2 seems to be directly related to the interaction between the electron deficient carbon (the Lewis acid) of CO_2 and the nitro group oxygen (the Lewis base) of PNA.

Despite small structural deformation in the moieties of these complexes, there is considerable charge redistribution in PNA and CO_2 upon complexation (see Figure 2). The population analysis of complexes **I** and **II** using the MP2 charge density reveals the electron-donating character of the nitro group oxygen to the electron-deficient carbon of CO_2, characterizing a kind of LA−LB interaction in these complexes. This charge redistribution is also demonstrated by comparing the calculated

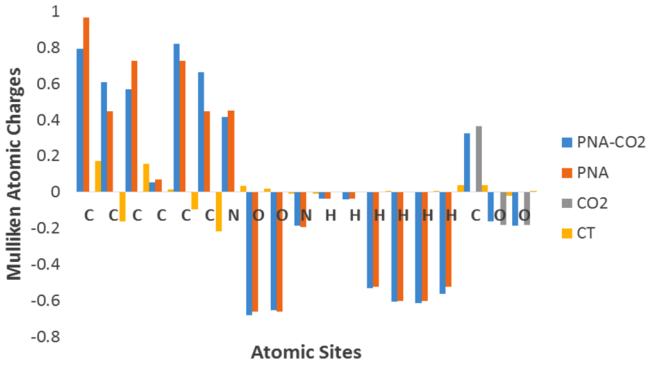

Figure 2. Charge distribution and charge transfer (CT) in the atomic sites of the PNA–CO_2 complex, in comparison with the isolated moieties, calculated using the MP2 density.

dipole moment for each complex with the corresponding value calculated for PNA. The calculated dipole moment of the ground state with MP2/aug-cc-pVDZ of PNA is 6.16 D, which is in very good agreement with the experimental value of 6.2 D, obtained by dielectric methods.[49] Upon complexation, we obtain a small reduction in the dipole moment of 0.04 D in complex **I** and of 0.08 D in complex **II**, indicating a charge separation in PNA. This is displayed in Figure 2, from which we notice that the bound CO_2 molecules also undergo a small charge redistribution. All of these changes reflect moderate interaction energies of −3.71 kcal/mol in complex **I** and −7.44 kcal/mol in complex **II**, as given in Table 2. However, due to

Table 2. Interaction, Counterpoise Correction, and Zero-Point Vibrational Energies (in kcal/mol) Calculated at the MP2/aug-cc-pVDZ Level for the PNA-CO_2 Complexes

energies	complex **I**	complex **II**
ΔE	−3.71	−7.44
ΔE^{cp}	−2.25	−4.46
ΔZPVE	1.41	2.84

their cooperative character[37] discussed here, it is difficult to assign separate energies to the individual contributions (LA–LB and H-bond). Even considering the zero-point vibration energy corrections, these complexes are shown to be stable with respective complexation energies of −2.30 and −4.60 kcal/mol. Regarding the BSSE corrections, the calculated interaction energies (ΔE^{cp}) are −2.25 kcal/mol for complex **I** and −4.46 kcal/mol for complex **II** (see Table 2), which really confirm that these complexes are weakly bound systems. The present values are in accordance with the complexation energy of other LA–LB complexes studied before.[10,12]

It is more instructive analyzing the formation of these complexes from the changes in their vibrational spectra, since experimentally[7] IR and Raman spectroscopies have been employed to identify other weakly bound complexes. In this sense, we have calculated the IR and Rama spectra, as well as depolarized light scattering properties for specific vibrational modes directly involved in the intermolecular interaction. The calculated vibrational modes along with their corresponding shifts are given in Table 3. Particularly interesting in describing the CO_2 complexes with PNA, the symmetric NO_2 stretching mode, $\nu_s(NO_2)$, exhibits the most intense band both in the Raman and in the IR spectra (see Figure 3). This mode is characterized by the delocalization over the whole π system,

Table 3. Specific Vibrational Modes and Corresponding Shifts (in cm^{-1}) Calculated at the MP2/aug-cc-pVDZ Level

assignment	PNA			
stretching	exptl.[a]	theory	complex **I**	complex **II**
$\nu_s(NO_2)$	1325	1397.3	1399.6	1401.7
$\Delta\nu s(NO_2)^b$			+2.3	+4.4
$\nu_{as}(NO_2)$	1587	1737.2	1731.2	1726.0
$\Delta\nu as(NO_2)^b$			−6.0	−11.2
ν_s(C–H)		3251.7	3251.1	3263.2
$\Delta\nu_s$(C–H)			−0.1	+11.5
ν_{as}(C–H)		3251.7	3263.4	3263.8
$\Delta\nu_{as}$(C–H)			+11.7	+12.1
scissoring	exptl.[a]	theory	complex **I**	complex **II**
$\delta_s(NH_2)$	1636	1661.9	1661.5	1661.3
$\delta_s(NH_2)$, ν(C–C)	1600	1634.8	1634.4	1633.9

[a]Refs 22, 50, 53. [b]Because of LA–LB or H-bond complexation.

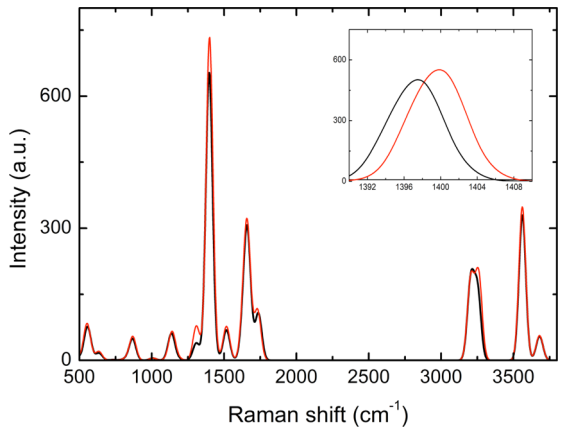

Figure 3. Calculated Raman spectra of PNA (black line) and PNA–CO_2 (red line) at the MP2/aug-cc-pVDZ level. The inset shows the blue shift in the $\nu_s(NO_2)$ mode upon CO_2 complexation.

albeit with a predominance of the C–NO_2 stretching,[23] and is also recognized as strongly solvent dependent, in contrast to other vibrational modes that usually undergo only minor changes.[20] As reported earlier,[17,21] the large resonance Raman activity of $\nu_s(NO_2)$ exerts strong influence on the electronic absorption band shape. Consequently, changes in the electronic absorption spectrum may be investigated via specific coupling of $\nu_s(NO_2)$ with the solvent.

In general, the $\nu_s(NO_2)$ mode in PNA exhibits a pronounced vibrational solvatochromism.[51] As demonstrated by Dreyer et al.,[23] the frequency of this band decreases with increasing polarity of the solvent mixtures. For instance, the observed red shift between CCl_4 and DMSO–D_6 solutions amounts to 26 cm^{-1}, while the shift between CCl_4 and toluene solutions is only 4 cm^{-1}. On the contrary, within MP2/aug-cc-pVDZ calculations for complexes **I** and **II**, we have found small blue shifts in the $\nu_s(NO_2)$ mode of 2.3 and of 4.4 cm^{-1}, respectively, from the isolated PNA molecule. This behavior is, however, compatible with other weakly bound systems.[52] It is worth mentioning here that considering density-functional-theory calculations, such as B3LYP/aug-cc-pVDZ, we obtain only a very small red shift of 0.7 cm^{-1} for this vibrational mode in complex **I**. In addition, analyzing the asymmetric NO_2 stretching mode, $\nu_{as}(NO_2)$—a moderately intense band both in the Raman and IR spectra—we obtain within MP2 red shifts of 6 and 11.2 cm^{-1}, respectively, for complex **I** and complex **II**.

dx.doi.org/10.1021/ct401081e | J. Chem. Theory Comput. 2014, 10, 1554–1562

Indeed, the calculated frequency of $\nu_{as}(NO_2)$ appears to be overestimated within MP2/aug-cc-pVDZ, which gives a value of 1737.2 cm^{-1} for isolated PNA, as compared to the experimental result[23] of 1587 cm^{-1} and the B3LYP/aug-cc-pVDZ value of 1568.6 cm^{-1}. Now considering the B3LYP level, we obtain a smaller red shift of 3 cm^{-1} for this vibrational mode in complex **I**. We notice, however, that changes in the vibrational spectra of the CO_2 complexes of PNA calculated with B3LYP seem to be less meaningful in comparison to MP2. This is not surprising, since these complexes are weakly bound and high-level electron correlation may be important to describe the intermolecular interactions as well as the electronic structure in these complexes.[52]

A secondary effect, but still important in the vibrational spectra of these LA−LB complexes, becomes evident because of the nonconventional H-bond formed with a first neighbor hydrogen to the nitro group in the aromatic ring of PNA and that of the oxygen atoms of CO_2 (see Figure 1), acting cooperatively in the complexation. For this reason, the symmetric CH stretching mode, ν_s(C−H), involved in the C−H···O bond undergoes a large blue shift of 11.5 cm^{-1} in complex **II**, although no meaningful change occurs for this mode in complex **I**. Moreover, in the case of the asymmetric CH stretching mode, ν_{as}(C−H), large blue shifts of 11.7 and 12.1 cm^{-1} are calculated in both complexes, as given in Table 3. Another characteristic vibrational change accompanying the LA−LB complexation with CO_2 is the splitting in its ν_2 mode. As reported in Table 4, the degeneracy of this bending mode is lifted in both complexes. This effect originates from the interaction between the electron deficient carbon of CO_2 and the nitro group oxygen of PNA in the same plane of the complex. The MP2 calculated splitting for complex **I** is 7.1 cm^{-1}, although exhibiting a small absorption in the IR spectrum and negligible intensity in the Raman spectrum. In the case of complex **II**, because of the presence of two bound CO_2 molecules, this splitting is still separated because of the symmetric and asymmetric combined ν_2 modes (see Table 4). As expected, this splitting gives a good indication of the complex formation, but none of them exhibits appreciable Raman activities.

Table 4. Bending Frequency[a] and Splitting (in cm^{-1}) in the CO_2 Molecule upon Complexation Calculated at the MP2/aug-cc-pVDZ Level

complexes	ν_2 splitting		$\Delta\nu_2$
complex **I**	646.7	654.3	7.6
complex **II**[b]	646.4 (647.6)	654.5 (654.6)	8.1 (7.0)

[a]The calculated frequency for the isolated CO_2 molecule is 655.6 cm^{-1}. [b]Values in parentheses refer to the symmetrically combined ν_2 mode of two CO_2 molecules.

As a complement to the Raman shift, it is also interesting to analyze the Raman light-scattering properties of the modes involved in the LA−LB complexation. Table 5 reports the calculated values of Raman intensities and depolarization ratios for PNA and its two complexes. For each vibrational mode considered, we report the intensity (A_n) and degree of depolarization of planar and natural incident light (ρ_p and ρ_n, respectively). From these results, it is clear that the symmetric NO_2 stretching mode exhibits the largest intensities among the selected modes, but it is only moderately depolarized with respect to the maxima depolarization ratios. Furthermore, there are no significant variations in ρ_p or ρ_n upon complexation with CO_2. In turn, the asymmetric NO_2 stretching is the most depolarized mode in these complexes, exhibiting maxima values of Raman depolarization ratios (ρ_p = 0.75 and ρ_n = 0.86), accordingly to the Raman light scattering. On the contrary, the least depolarized mode among these selected modes of PNA is ν_s(C−H), with ρ_p = 0.13 and ρ_n = 0.24. Moreover, the depolarization of ν_s(C−H) slightly increases to ρ_p = 0.17 and ρ_n = 0.29 upon the C−H···O bond formation in complex **I**. Most interestingly, ν_{as}(C−H) is highly depolarized in isolated PNA (ρ_p = 0.71 and ρ_n = 0.83) but yields the largest variations upon complexation with one CO_2 molecule, giving ρ_p = 0.23 and ρ_n = 0.37. This reduction in the depolarization ratios may be useful to identify the LA−LB complexation of PNA with CO_2.

3.2. Electronic Absorption Spectra of PNA and Its Complexes in $SCCO_2$. To describe the electronic excitations of PNA, which is a prototypical "push−pull" molecule, one usually considers a combination of neutral and zwitterionic charge-transfer (CT) resonance structures.[17] Recently, Narra et al.[53] have proposed a partial quinoid structure to explain the lowest excited triplet (T1) state of PNA in acetonitrile. However, in its lowest singlet $\pi \rightarrow \pi^*$ CT absorption the ground state is dominated by the neutral form, whereas the excited state presents a considerable contribution of the CT form (Figure 4). This is in line with the large increase, of about 9 D, observed in the dipole moment from the ground state to the lowest singlet state.[49] Considering an isolated PNA molecule, we have calculated a vertical excitation energy of 4.31 eV using TD-CAM-B3LYP/aug-cc-pVDZ (with the MP2/aug-cc-pVDZ optimized geometry), whereas the experimental value[27] for the corresponding excitation is 4.24 eV (see Table 6).

As in the case of the vibrational spectra of PNA, its CT electronic absorption is also strongly dependent on the solvent. Because of the high polarity of PNA, it is expected that the solvatochromic shift of the electronic CT band increases with the increasing polarity of the solvent. However, for PNA in $SCCO_2$, a small shift in the CT absorption band is expected since CO_2 is a nonpolar solvent. The experimental data[28] in $SCCO_2$ for different densities have shown absorbance maxima

Table 5. Raman Intensities (in $Å^4$/amu) and Depolarization Ratios Related to Plane-Polarized and Natural Incident Light Calculated at the MP2/aug-cc-pVDZ Level

	PNA			complex **I**			complex **II**		
mode	A_n	ρ_p	ρ_n	A_n	ρ_p	ρ_n	A_n	ρ_p	ρ_n
$\nu_s(NO_2)$	653	0.24	0.38	734	0.23	0.37	824	0.22	0.36
$\nu_{as}(NO_2)$	107	0.75	0.86	114	0.75	0.86	122	0.75	0.86
ν_s(C−H)	138	0.13	0.24	80	0.17	0.29	188	0.12	0.21
ν_{as}(C−H)	17	0.71	0.83	121	0.23	0.37	56	0.75	0.86

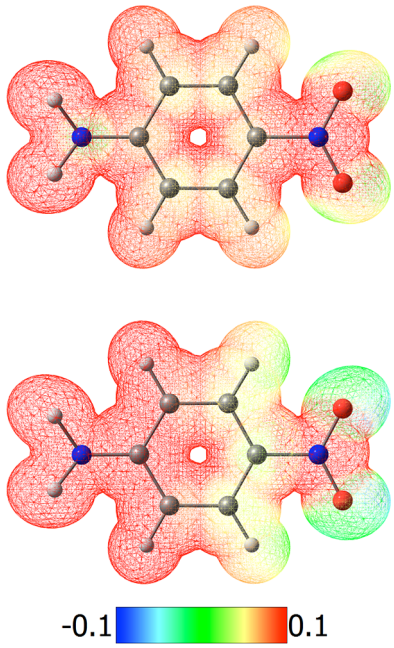

Figure 4. Electrostatic potential (in a.u.) calculated with MP2/aug-cc-pVDZ for the neutral (top) and zwitterionic (bottom) forms of PNA.

Table 6. Vertical Excitation Energies (in eV) for the Lowest Singlet $\pi \rightarrow \pi^*$ CT Absorption Calculated at the TD-CAM-B3LYP/aug-cc-pVDZ Level, Within the S-QM/MM Method for PNA in $SCCO_2$

	PNA in the gas phase		PNA in supercritical CO_2		
	theory	exptl.	PNA + 350 PC	PNA+ 12 CO_2 + 350 PC	exptl.
$\pi \rightarrow \pi^*$	4.31	4.24	4.22 ± 0.01	4.13 ± 0.02	3.89
shift			−0.09 ± 0.01	−0.18 ± 0.02	−0.35

near 3.89 eV, which corresponds to a solvatochromic red shift of 0.35 eV (2823 cm^{-1}) going from the gas phase. This variation, however, is surprisingly higher as compared to the measured shifts of the electronic CT bands of PNA in binary mixtures with different polarities.[23] For example, the electronic shifts vary about 1300 cm^{-1} between CCl_4 and toluene, while the shift between CCl_4 and DMSO−D_6 is about 5000 cm^{-1}, according to experiments carried out by Dreyer and Werncke.[23]

To better understand this problem, we have initially taken into account the isolated PNA molecule in a polarizable continuum model to represent the $SCCO_2$, which corresponds to a dielectric constant ε = 1.5. As given in Table 7, our calculated excitation energy value with TD-CAM-B3LYP/aug-cc-pVDZ (within the MP2/aug-cc-pVDZ optimized geometry in PCM) is now 4.13 eV, corresponding to a red shift of 0.18 eV (1452 cm^{-1}). Despite possible deficiencies of LC-DFT calculations to reproduce absorption spectra, it is also expected from the PCM approach, without considering explicit solvent molecules, that the calculated shift at this level should be underestimated in low polarity solvents, as compared to the experimental value of 0.35 eV (see Table 7).

Table 7. Vertical Excitation Energies (in eV) for the Lowest Singlet $\pi \rightarrow \pi^*$ CT Absorption Calculated at the TD-CAM-B3LYP/aug-cc-pVDZ for PNA and its Complexes I and II in $SCCO_2$ (PCM)

	PNA	complex **I**	complex **II**	exptl.
$\pi \rightarrow \pi^*$	4.13	4.08	4.03	3.89
shift	−0.18[a]	−0.23	−0.28	−0.35

[a]From PNA in the gas phase.

In the next step, we have considered statistically uncorrelated configurations obtained from an MC simulation performed for one PNA molecule in 500 CO_2 molecules within supercritical conditions. From our S-QM/MM scheme, we have considered two situations: (i) one PNA within an embedding of 350 CO_2 molecules treated as point charges (PC) representing the solvent molecules and (ii) one PNA plus 12 CO_2 molecules within an embedding of 350 CO_2 molecules treated as point charges. In Figure 5a, we illustrate the explicit molecules in the first solvation shell of PNA in $SCCO_2$. Although there is clear evidence of aggregation of CO_2 around the solute, as demonstrated by the radial distribution function (RDF) displayed in Figure 5b, it gives no evidence of specific interactions formed around the nitro group of PNA.

The calculated average shifts for the different levels i and ii are reported in Table 6. As can be seen, the effect of a purely electrostatic embedding amounts to a red shift of only 0.09 eV, whereas the inclusion of 12 CO_2 molecules belonging to the first solvation shell of PNA increases this shift to 0.18 eV. We notice, however, that this value is well comparable to the shift calculated with one PNA molecule in PCM. This result means that the effect of explicit CO_2 molecules, even considering the supercritical conditions during the simulation, is not enough to describe the red shift of the $\pi \rightarrow \pi^*$ CT band in $SCCO_2$. In practice, the classical model[48] employed for CO_2 could hardly describe quantum chemical interactions such as LA−LB interactions. Thus, possible effects in the electronic spectrum due to specific interactions between PNA and CO_2 may be assessed via a detailed microsolvation analysis.

As reported here, we have demonstrated that PNA, possessing an electron-donating functional group, may exhibit specific interactions with CO_2, most probably of Lewis acid−base nature. In this sense, LA−LB interactions may be sufficiently long-lived to influence the intramolecular CT electronic transition of PNA. Consequently, upon complexation with CO_2, a relatively higher red shift in the absorption band of PNA, compared to its gas phase, should be expected in the electronic spectrum. Therefore, considering the calculated vertical excitation energies of complexes **I** and **II**, at the TD-CAM-B3LYP/aug-cc-pVDZ level in PCM (ε = 1.5), we obtain significant increases in the lowest singlet $\pi \rightarrow \pi^*$ CT absorption band of PNA (see Table 7). For example, considering complex **I**, the calculated red shift increases to 0.23 eV, which corresponds to 66% of the experimental data, whereas considering complex **II**, this value increases to 0.28 eV, giving 80% of the experimental data. As complex **I** should be most probable to be formed in SCCO2, the failure of TDDFT in reproducing the solvatochromic shift should amount to 34%.

In Figure 6, we display the Kohn−Sham highest occupied molecular orbital (HOMO) and the lowest unoccupied molecular orbital (LUMO) of both complexes, as obtained with TD-CAM-B3LYP(PCM)/aug-cc-pVDZ and optimized structures with MP2(PCM)/aug-cc-pVDZ. Differently from those observed for LA−LB complexes of CO_2 with carbonyl groups,[12] the HOMO and LUMO of the PNA-CO_2 complexes essentially remain delocalized in the PNA molecule. At this level of calculation, the LUMO energy of the PNA molecule in

dx.doi.org/10.1021/ct401081e | J. Chem. Theory Comput. 2014, 10, 1554−1562

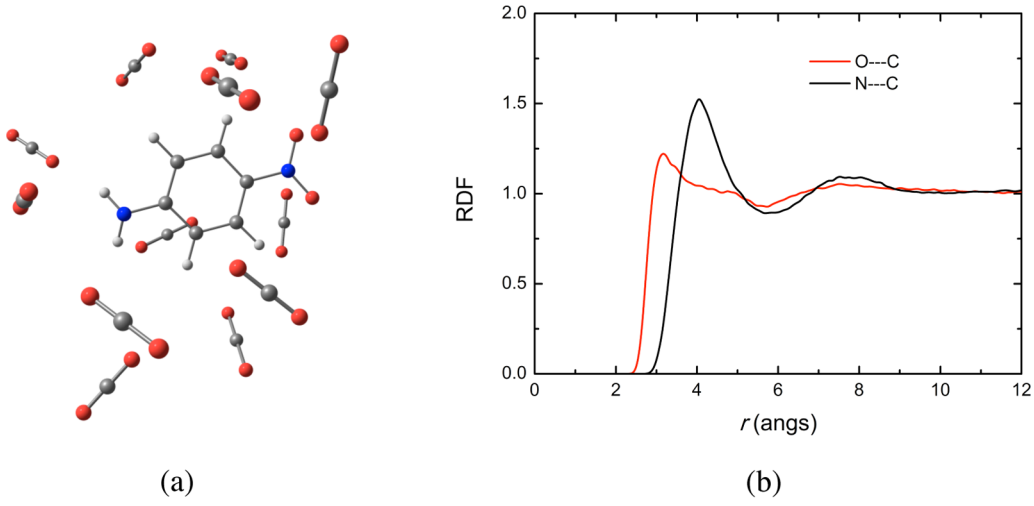

Figure 5. (a) Illustration of one configuration of PNA in $SCCO_2$ containing 12 molecules of CO_2 obtained from the MC simulation. (b) Radial distribution function (RDF) of CO_2 carbon atoms around the nitro group of PNA.

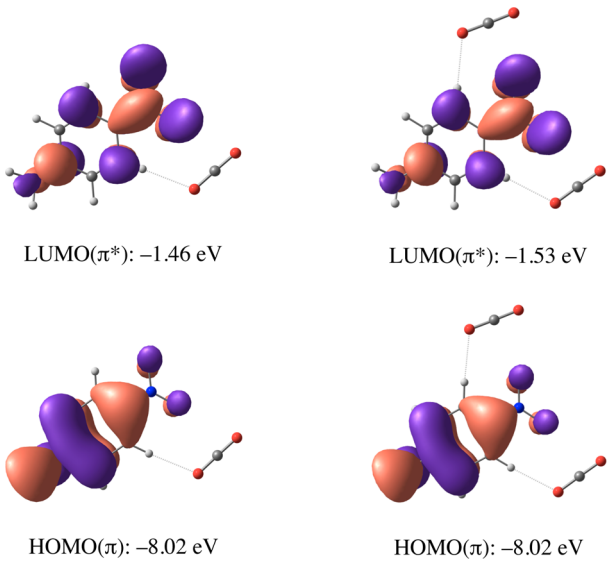

Figure 6. Kohn–Sham frontier molecular orbitals of the dominant linear response transition vector for the lowest singlet $\pi \rightarrow \pi^*$ CT excitation of the LA–LB complexes of PNA, calculated at TD-CAM-B3LYP/aug-cc-pVDZ.

PCM is −1.40 eV, whereas it is shifted to −1.46 eV in complex **I** and −1.53 eV in complex **II**. However, the main effect of the CO_2 molecule is inducing charge redistribution in PNA, which appears to be responsible for the high red shift observed in its $\pi \rightarrow \pi^*$ intramolecular CT excitation, from the gas phase.

4. SUMMARY AND CONCLUSIONS

In this work, based on recent experimental studies of PNA in $SCCO_2$, we have employed ab initio quantum chemical methods to carry out a theoretical prediction of the possible existence of a specific interaction between PNA and CO_2, which can account for the unusual solvatochromism of PNA. The solute–solvent interaction was supposed to be of the Lewis acid–base nature. The resulting geometries and binding energies of PNA–CO_2 complexes also suggest the existence of a C–H···O interaction between a first neighbor hydrogen atom, relative to the nitro group in the aromatic ring of PNA, and one of the oxygen atoms of CO_2. Also, Raman spectroscopic properties of the proposed complexes are in line with the LA–LB interactions. Other evidence of this complexation is the observation of the splitting of the vibrational mode ν_2 in the CO_2 molecule. This splitting indicates that the double degeneracy of this mode is removed due to the interaction of electron lone pairs of the nitro oxygen with the carbon atom of the CO_2 molecule.

Experimentally, our theoretical contention may be supported by the relatively strong $\pi \rightarrow \pi^*$ absorption band in the near-UV–vis spectral region observed for PNA in $SCCO_2$. In this direction, we have performed an S-QM/MM simulation under supercritical conditions to evaluate the lowest singlet excitation of PNA within LC TD-DFT. The results show that the inclusion of 12 CO_2 molecules, belonging to the first solvation shell of PNA, within an embedding of 350 CO_2 molecules treated as point charges representing the solvent molecules, gives an average shift of 0.18 ± 0.02 eV. This value corresponds to only 51% of the experimental data. As expected, the structures of $SCCO_2$ obtained from a classical simulation could hardly describe quantum chemical interactions such as LA–LB interactions. However, considering formation of PNA-CO_2 complexes, we have obtained significant increases in the solvatochromic shift of lowest excitation of PNA. Our calculated red shift from the gas phase accounts for 66% to 80%, depending on the degree of complexation, of the experimental data. These results thus alleviate the failure commonly attributed to LC TD-DFT in reproducing the solvatochromic shift of the lowest CT excitation in PNA.

AUTHOR INFORMATION

Corresponding Authors

*E-mail: rivelino@ufba.br.
*E-mail: canuto@if.us.br.

Notes

The authors declare no competing financial interest.

ACKNOWLEDGMENTS

This work has been partially supported by CNPq, CAPES, NAP-FCx, and FAPESP (Brazil).

REFERENCES

(1) Eckert, C. A.; Knutson, B. L.; Debendetti, P. G. Supercritical Fluids as Solvents for Chemical and Materials Processing. *Nature* **1996**, *383*, 313−318.

(2) Xynos, N.; Papaefstathiou, G.; Psychis, M.; Argyropoulou, A.; Aligiannis, N.; Skaltsounis, A.-L. Development of a Green Extraction Procedure with Super/Subcritical Fluids to Produce Extracts Enriched in Oleuropein from Olive Leaves. *J. Supercrit. Fluids* **2012**, *67*, 89−93.

(3) Eric, J. Beckman. Supercritical and Near-Critical CO_2 in Green Chemical Synthesis and Processing. *J. Supercrit. Fluids* **2004**, *28*, 121−191.

(4) Long, J. J.; Ma, Y. Q.; Zhao, J. P. Investigations on the Level Dyeing of Fabrics in Supercritical Carbon Dioxide. *J. Supercrit. Fluids* **2011**, *57*, 80−86.

(5) Jin, J. S.; Ning, Y. Y.; Hu, K.; Wu, H.; Zhang, Z. T. Solubility of p-Nitroaniline in Supercritical Carbon Dioxide with and without Mixed Cosolvents. *J. Chem. Eng. Data* **2013**, *58*, 1464−1469.

(6) Reilly, J. T.; Bokis, C. P.; Donohue, M. D. An Experimental Investigation of Lewis Acid-Base Interactions of Liquid Carbon-Dioxide Using Fourier-Transform Infrared (FT-IR) Spectroscopy. *Int. J. Thermophys.* **1995**, *16*, 599−610.

(7) Blatchford, M. A.; Raveendran, P.; Wallen, S. L. Raman Spectroscopic Evidence for Cooperative C-H···O Interactions in the Acetaldehyde-CO_2 Complex. *J. Am. Chem. Soc.* **2002**, *124*, 14818−14819.

(8) Kobatake, Y.; Hildebrand, J. H. Solubility and Entropy of Solutions of He, N_2, A, O_2, CH_4, C_2H_6, CO_2 and SF_6 in Various Solvents; Regularity of Gas Solubilities. *J. Phys. Chem.* **1961**, *65*, 331−335.

(9) Kazarian, S. G.; Vincent, M. F.; Bight, F. V.; Liotta, C. L.; Eckert, C. A. Specific Intermolecular Interaction of Carbon Dioxide with Polymers. *J. Am. Chem. Soc.* **1996**, *118*, 1729−1736.

(10) Raveendran, P.; Wallen, S. L. Cooperative C-H···O Hydrogen Bonding in CO_2 Lewis Base Complexes: Implications for Solvation in Supercritical CO_2. *J. Am. Chem. Soc.* **2002**, *124*, 12590−12599.

(11) Raveendran, P.; Wallen, S. L. Sugar Acetates as Novel, Renewable CO_2-philes. *J. Am. Chem. Soc.* **2002**, *124*, 7274−7275.

(12) Rivelino, R. Lewis Acid-Base Interactions in Weakly Bound Formaldehyde Complexes with CO2, HCN, and FCN: Considerations on the Cooperative H-Bonding Effects. *J. Phys. Chem. A* **2008**, *112*, 161−165.

(13) Trung, N. T.; Nguyen, M. T. Interactions of Carbon Dioxide with Model Organic Molecules: A Comparative Theoretical Study. *Chem. Phys. Lett.* **2013**, *518*, 10−15.

(14) Altarsha, M.; Ingrosso, F.; Ruiz-Lopez, M. F. A New Glimpse into the CO_2 Philicity of Carbonyl Compounds. *ChemPhysChem* **2012**, *13*, 3397−3403.

(15) Foltran, S.; Méreau, R.; Tassaing, T. On the Interaction Between Supercritical CO_2 and Epoxides Combining Infrared Absorption Spectroscopy and Quantum Chemistry Calculations. *Phys. Chem. Chem. Phys.* **2011**, *13*, 9209−9215.

(16) Garza, A. J.; Scuseria, G. E.; Khan, S. B.; Asiri, A. M. Assessment of Long-Range Corrected Functionals for the Prediction of Non-Linear Optical Properties of Organic Materials. *Chem. Phys. Lett.* **2013**, *575*, 122−125.

(17) Moran, A. M.; Kelley, A. M. Solvent Effects on Ground and Excited Electronic State Structures of p-Nitroaniline. *J. Chem. Phys.* **2001**, *115*, 912−924.

(18) Chiş, V.; Monica, M.; Venter, M. M.; Leopold, N.; Cozar, O. R. Surface-Enhanced Raman Scattering and DFT Study of Para-Nitro-Aniline. *Vibration Spectrosc.* **2008**, *48*, 210−214.

(19) Tomotsumi, F.; Masahide, T.; Yoshifumi, K. Solvent Effects on the Local Structure of p-Nitroaniline in Supercritical Water and Supercritical Alcohols. *J. Phys. Chem. A* **2008**, *112*, 5515−5526.

(20) Wang, C.-K.; Wang, Y.-H. Solvent Dependence of Solvatochromic Shifts and the First Hyperpolarizability of para-Nitroaniline: A Nonmonotonic Behavior. *J. Chem. Phys.* **2003**, *119*, 4409−4412.

(21) Schmid, E. D.; Moschallski, M.; Peticolas, W. L. Solvent Effects on the Absorption and Raman Spectra of Aromatic Nitro Compounds. 1. Calculation of Preresonance Raman Intensities. *J. Phys. Chem.* **1986**, *90*, 2340−2346.

(22) Kozich, V.; Werncke, W.; Dreyer, J.; Brzezinka, K.-W.; Rini, M.; Kummrow, A.; Elsaesser, T. Vibrational Excitation and Energy Redistribution after Ultrafast Internal Conversion in 4-Nitroaniline. *J. Chem. Phys.* **2002**, *117*, 719−725.

(23) Dreyer, J.; Kozich, V.; Werncke, W. Tuning Intramolecular Anharmonic Vibrational Coupling in 4-Nitroaniline by Solvent-Solute Interaction. *J. Chem. Phys.* **2007**, *127*, 234505.

(24) Sok, S.; Willow, S. Y.; Zahariev, F.; Gordon, M. S. Solvent-Induced Shift of the Lowest Singlet $\pi\rightarrow\pi^*$ Charge-Transfer Excited State of p-Nitroaniline in Water: An Application of the TDDFT/EFP1Method. *J. Phys. Chem. A* **2011**, *115*, 9801−9809.

(25) Dmytro Kosenkov, D.; Slipchenko, L. V. Solvent Effects on the Electronic Transitions of p-Nitroaniline: A QM/EFP Study. *J. Phys. Chem. A* **2011**, *115*, 392−401.

(26) Eriksen, J. J.; Sauer, S. P. A.; Mikkelsen, K. V.; Christiansen, O.; Jensen, H. J. A.; Kongsted, J. Failures of TDDFT in Describing the Lowest Intramolecular Charge-Transfer Excitation in para-Nitroaniline. *Mol. Phys.* **2013**, *111*, 1235−1248.

(27) Frutos-Puerto, A.; Aguilar, M. A.; Galván, I. F. Theoretical Study of the Preferential Solvation Effect on the Solvatochromic Shifts of para-Nitroaniline. *J. Phys. Chem. B* **2013**, *117*, 2466−2474.

(28) Sigman, M. E.; Lindley, S. M.; Leffler, J. E. Supercritical Carbon Dioxide: Behavior of π^* and β Solvatochromic Indicator in Media of Different Densities. *J. Am. Chem. Soc.* **1985**, *107*, 1471−1472.

(29) Millefiori, S.; Favini, G.; Millefiori, A.; Grasso, D. Electronic-Spectra and Structure of Nitroanilines. *Spectrochim. Acta* **1977**, *33A*, 21−27.

(30) Modesto-Costa, L.; Coutinho, K.; Mukherjee, P. K.; Canuto, S. Combining Monte Carlo Simulation and Density-Functional Theory to Describe the Spectral Changes of Na_2 in Liquid Helium. *Phys. Rev. A* **2011**, *83*, 042515.

(31) Fonseca, T. L.; Coutinho, K.; Canuto, S. Hydrogen Bond Interactions Between Acetone and Supercritical Water. *Phys. Chem. Chem. Phys.* **2010**, *12*, 6660−6665.

(32) Hidalgo, M.; Canuto, S. A Theoretical Study of the Spectral Shifts of Xe Atom in Ar Environment. *Phys. Lett. A* **2013**, *377*, 1720−1724.

(33) Mota, F.; de, B.; Rivelino, R. Optical Response of Liquid Acetonitrile at Ambient Conditions: The Dynamical Dielectric Behavior from Ab Initio Calculations. *J. Phys. Chem. B* **2009**, *113*, 9489−9492.

(34) Rivelino, R.; Coutinho, K.; Canuto, S. A Monte Carlo-Quantum Mechanics Study of the Solvent-Induced Spectral Shift and the Specific Role of Hydrogen Bonds in the Conformational Equilibrium of Furfural in Water. *J. Phys. Chem. B* **2002**, *106*, 12317−12322.

(35) Orozco-Gonzalez, Y.; Bistafa, C.; Canuto, S. Solvent Effect on the Stokes Shift and on the Nonfluorescent Decay of the Daidzein Molecular System. *J. Phys. Chem. A* **2013**, *117*, 4404−4411.

(36) Head-Gordon, M.; Pople, J. A.; Frisch, M. J. MP2 Energy Evaluation by Direct Methods. *Chem. Phys. Lett.* **1988**, *153*, 503−506.

(37) Frisch, M. J.; Trucks, G. W.; Schlegel, H. B.; Scuseria, G. E.; Robb, M. A.; Cheeseman, J. R.; Scalmani, G.; Barone, V.; Mennucci, B.; Petersson, G. A.; Nakatsuji, H.; Caricato, M.; Li, X.; Hratchian, H. P.; Izmaylov, A. F.; Bloino, J.; Zheng, G.; Sonnenberg, J. L.; Hada, M.; Ehara, M.; Toyota, K.; Fukuda, R.; Hasegawa, J.; Ishida, M.; Nakajima, T.; Honda, Y.; Kitao, O.; Nakai, H.; Vreven, T.; Montgomery, J. A., Jr.; Peralta, J. E.; Ogliaro, F.; Bearpark, M.; Heyd, J. J.; Brothers, E.; Kudin, K. N.; Staroverov, V. N.; Kobayashi, R.; Normand, J.; Raghavachari, K.; Rendell, A.; Burant, J. C.; Iyengar, S. S.; Tomasi, J.; Cossi, M.; Rega, N.; Millam, J. M.; Klene, M.; Knox, J. E.; Cross, J. B.; Bakken, V.; Adamo, C.; Jaramillo, J.; Gomperts, R.; Stratmann, R. E.; Yazyev, O.; Austin, A. J.; Cammi, R.; Pomelli, C.; Ochterski, J. W.; Martin, R. L.; Morokuma, K.; Zakrzewski, V. G.; Voth, G. A.; Salvador, P.; Dannenberg, J. J.; Dapprich, S.; Daniels, A. D.; Farkas, O.; Foresman, J. B.; Ortiz, J. V.; Cioslowski, J.; Fox, D. J. *Gaussian 09*, revision A.02; Gaussian Inc.: Wallingford, CT, 2009.

(38) Kendall, R. A.; Dunning, T. H., Jr.; Harrison, R. J. Electron Affinities of the First-Row Atoms Revisited. Systematic Basis Sets and Wave Functions. *J. Chem. Phys.* **1992**, *96*, 6796−6806.
(39) Scheiner, S. *Hydrogen Bonding: A Theoretical Perspective*; Oxford University Press: New York, 1997.
(40) van Duijneveldt, F. B.; van Duijneveldt-van de Rijdt, J. G. C. M.; van Lente, J. H. State of the Art in Counterpoise Theory. *Chem. Rev.* **1994**, *94*, 1873−1885.
(41) Szymanski, H. A. *Raman Spectroscopy*; Plenum Press: New York, 1967.
(42) Koch, W.; Holthausen, M. C. *A Chemist's Guide to Density Functional Theory*; Wiley-VCH: Weinheim, German, 2001.
(43) Runge, E.; Gross, E. K. U. Density-Functional Theory for Time-Dependent Systems. *Phys. Rev. Lett.* **1984**, *52*, 997−1000.
(44) Casida, M. E. In *Time-Dependent Density-Functional Response Theory for Molecules*; Chong, D. P., Ed.; World Scientific: Singapore, 1995; Vol. *1*, pp 155−192.
(45) Charaf-Eddin, A.; Planchat, A.; Mennucci, B.; Carlo Adamo, C.; Jacquemin, D. Choosing a Functional for Computing Absorption and Fluorescence Band Shapes with TD-DFT. *J. Chem. Theory Comput.* **2013**, *9*, 2749−2760.
(46) Scalmania, G.; Frisch, M. J.; Mennucci, B.; Tomasi, J.; Cammi, R.; Barone, V. Geometries and Properties of Excited States in the Gas Phase and in Solution: Theory and Application of a Time-Dependent Density Functional Theory Polarizable Continuum Model. *J. Chem. Phys.* **2006**, *124*, 094107.
(47) Wesch, A.; Dahmen, N.; Ebert, K. H. Measuring the Static Dielectric Constants of Pure Carbon Dioxide and Carbon Dioxide Mixed with Ethanol and Toluene at Elevated Pressures. *Ber. Bunsen Phys. Chem.* **1996**, *100*, 1368−1371.
(48) Zhang, Z.; Duan, Z. An Optimized Molecular Potential for Carbon Dioxide. *J. Chem. Phys.* **2005**, *122*, 214507.
(49) Sinha, H. K.; Yates, K. On the Ground and Excited State Dipole Moments of Planar vs. Twisted Nitroaniline Analogues. *Can. J. Chem.* **1991**, *69*, 550−557.
(50) Kozich, V.; Werncke, W.; Vodchits, A. I.; Dreyer, J. Ultrafast Excitation of out-of-plane Vibrations and Vibrational Energy Redistribution after Internal Conversion of 4-Nitroaniline. *J. Chem. Phys.* **2003**, *118*, 1808−1814.
(51) Dreyer, J.; Kozich, V.; Werncke, W. Tuning Intramolecular Anharmonic Vibrational Coupling in 4-Nitroaniline by Solvent-Solute Interaction. *J. Chem. Phys.* **2007**, *127*, 234505.
(52) Li, X.; Liu, L.; Schlegel, H. B. On the Physical Origin of Blue-Shifted Hydrogen Bonds. *J. Am. Chem. Soc.* **2002**, *124*, 9639−9647.
(53) Narra, S.; Chang, S.-W.; Witek, H. A.; Shigeto, S. Is Our Way of Thinking about Excited States Correct? Time-Resolved Dispersive IR Study on p-Nitroaniline. *Chem.—Eur. J.* **2012**, *18*, 2543−2550.